Proc. Natl. Acad. Sci. USA
Vol. 91, pp. 11621–11625, November 1994
Biochemistry

Three-dimensional structure of extended chromatin fibers as revealed by tapping-mode scanning force microscopy

(chicken erythrocytes/modeling)

SANFORD H. LEUBA*†, GUOLIANG YANG*†, CHARLES ROBERT‡, BRUNO SAMORI§, KENSAL VAN HOLDE‡, JORDANKA ZLATANOVA‡¶, AND CARLOS BUSTAMANTE‖**

*Institute of Molecular Biology, †Department of Chemistry, and ‖Howard Hughes Medical Institute, University of Oregon, Eugene, OR; ‡Department of Biochemistry and Biophysics, Oregon State University, Corvallis, OR 97331-7305; §Dipartimento di Chimica, Universita della Calabria, Arcavacata di Rende, Cosenza, Italy; and ¶Institute of Genetics, Bulgarian Academy of Sciences, 1113 Sofia, Bulgaria

Contributed by Kensal van Holde, June 22, 1994

ABSTRACT **Unfixed chicken erythrocyte chromatin fibers in very low salt have been imaged with a scanning force microscope operating in the tapping mode in air at ambient humidity. These images reveal a three-dimensional organization of the fibers. The planar "zig-zag" conformation is rare, and extended "beads-on-a-string" fibers are seen only in chromatin depleted of histones H1 and H5. Glutaraldehyde fixation reveals very similar structures. Fibers fixed in 10 mM salt appear somewhat more compacted. These results, when compared with modeling studies, suggest that chromatin fibers may exist as irregular three-dimensional arrays of nucleosomes even at low ionic strength.**

The structure of the chromatin fiber in low salt concentrations remains controversial. Electron microscopy (EM) experiments, most of which utilized the Miller spreading technique (1), typically showed extended "beads-on-a-string" or "open zig-zag" structures (refs. 2 and 3; for reviews, see refs. 4–6). At slightly higher ionic strength (≈10 mM NaCl), somewhat more compact, "closed" zig-zags of nucleosomes were observed (7–9). Only upon further addition of NaCl to about 100 mM did these extended structures condense to form the so-called 30-nm fiber (8), which resembles structures observed *in situ* (7, 9, 10). However, there has been concern that strong interactions of the fiber with the EM support surface, and the dehydration produced by the high vacuum conditions, could distort the structure, especially at low ionic strength.

Attempts to circumvent these problems used solution studies. The first scattering experiments suggested that the nucleosomes were densely packed in a linear array (11, 12). However, more recent results can be fitted better by an open-helix model (13–19). Unfortunately, none of these techniques can resolve details of structure, or provide more than average properties of heterogeneous fibers. More recently, cryo-EM suggested that the low-salt fiber exhibited some three-dimensional structure, although details of the conformation were difficult to resolve because of low contrast (reviewed in ref. 20). Furthermore, some earlier scanning transmission EM images may also be interpreted as two-dimensional projections of three-dimensional structures (19, 21).

To address this controversy, a study was performed using the three-dimensional imaging capabilities of a scanning force microscope, which makes it possible to image chromatin fibers under less damaging conditions (22, 23). The samples are never vacuum dried and are scanned in air at about 50% relative humidity. Under these conditions a film of liquid water resides on the support surface (24). The newly developed tapping operation mode (25, 26) was employed, in which a stiff cantilever is oscillated near its resonance frequency with amplitudes typically in the range of 10–20 nm as the sample is scanned laterally. The oscillation amplitude is kept constant via feedback control. This operation has several advantages over the contact mode, in which a tip is pulled across the sample. Tip–sample forces are lighter than in the contact mode. Moreover, since most of the force is perpendicular to the surface, the sample experiences minimal lateral deformation during scanning, thus improving spatial resolution (25, 26).

MATERIALS AND METHODS

Preparation and Fixation of Chromatin. Chicken erythrocyte chromatin was prepared essentially as described (27), with a reduction in the amount of micrococcal nuclease to allow isolation of long fibers (28). Soluble chromatin was dialyzed versus 5 mM triethanolamine/HCl (pH 7.0), with or without 10 mM NaCl and was stored on ice. In a few experiments, 10 mM Tris/HCl (pH 7.5) was used; the structures observed in Tris buffer were indistinguishable from those in triethanolamine buffer. When desired, chromatin was stripped of histones H1 and H5 (29).

Glutaraldehyde fixation of chromatin in the various salt concentrations was done as described (8, 30); the fixed preparations were dialyzed extensively versus triethanolamine buffer and were stored on ice.

Scanning Force Microscopy (SFM) Imaging. Fibers were deposited on cover glass cleaned by prebaking for 5 min at 600°C. Twenty microliters of sample was incubated on the glass surface for 1 min and rinsed with 10 drops of Nanopure water (Barnstad), and excess liquid was blotted and blown off with nitrogen gas. When freshly cleaved mica was used as a substrate, the surface was first treated with 20 μl of 1 nM spermidine for 5 min, washed, blotted, and dried with nitrogen gas. Spermidine treatment markedly improved adhesion to the mica. It is unlikely that the salt concentration of the samples increased during deposition, since hardly any evaporation occurred during the short incubation. Furthermore, after this incubation, the surface was thoroughly rinsed with water. Thus, the dissociation observed in 10 mM salt on mica (see *Results*) cannot have resulted from increasing salt concentration during the deposition process; similar dissociation was not observed on glass.

Analysis of SFM Images. The lateral dimensions of biological structures in SFM are overestimated because of the finite dimensions of the tips. Conversely, the heights are usually underestimated by an amount determined by the compliance of the sample, the minimal clipping of the cantilever ampli-

The publication costs of this article were defrayed in part by page charge payment. This article must therefore be hereby marked "*advertisement*" in accordance with 18 U.S.C. §1734 solely to indicate this fact.

Abbreviation: SFM, scanning force microscopy.

**To whom reprint requests should be addressed.

tude that yields stable imaging, and the strength of the attractive interaction between the tip and the sample. The tips used in the tapping mode have a pyramidal shape characterized by a taper angle θ. To a first approximation, the apparent lateral dimensions of an object can be related to the dimensions of the tip by

$$W_{app} = W_{true} + 2 \tan(\theta) H_{app}, \quad [1]$$

where W_{app} and W_{true} are the "apparent" and "true" widths of the object, respectively, and H_{app} is its apparent height. θ can be determined from the known width and the apparent width and height of nucleosomes in the same image. Once θ is known, the correct lateral dimensions of the object can be calculated from its apparent dimensions by using Eq. 1.

RESULTS

Chromatin Fibers Exhibit Three-Dimensional Structure in Dilute Buffers Even in the Absence of Added Salt. Fig. 1 shows SFM images of unfixed chicken erythrocyte chromatin fibers deposited on glass (*A* and *B*) and mica (*C* and *D*). The fibers are likely to retain at least the strongly bound and structurally essential water under the conditions used here (24). Irregular, three-dimensionally organized nucleosomal arrays are consistently observed in these preparations; only rarely can flat zig-zags or extended beads-on-a-string be found. The images on glass and mica are generally similar, although the mica surface appears to slightly extend unfixed fibers, perhaps because of stronger interaction with some chromatin components. The fibers have an apparent average diameter of about 44 ± 5 nm. This is certainly an overestimate, since in this series of experiments the objects corresponding to nucleosomes appear to be about 16 nm in diameter (Table 1). The measured diameter of nucleosomes can be used together with the expected value of 11 nm to estimate the correct lateral dimensions of the fibers (see *Materials and Methods*, Eq. 1). The corrected value for the unfixed fiber diameter then becomes 34 ± 5 nm (Table 1).

To eliminate possible distortions from interaction with the substrate, fibers fixed in glutaraldehyde were examined (Fig. 1 *E* and *F*, for examples on mica). These closely resemble unfixed fibers, except that the proportion of more regular three-dimensional structures increases slightly. The corrected fiber diameter remains essentially unchanged (34 ± 4 nm). Individual nucleosomes appear more well defined than in unfixed chromatin. This improvement may result from a reduced compliance of the fixed nucleosomes to tip forces. Similar images were obtained on glass (not shown).

The variation in color tones in Fig. 1 displays roughly the difference in height of different nucleosomes above the surface of the support. Although the SFM technique does not give absolute height values (see *Materials and Methods*), the fact that individual nucleosomes and fibers give apparent average heights of 3 nm and 6 nm, respectively, further supports the notion of a three-dimensional organization of these fibers. The three-dimensional nature of these structures is better depicted in surface plots seen from an inclination angle of 30° with respect to the horizon (Fig. 2).

This three-dimensional structure is not observed with chromatin depleted of histones H1 and H5 (Fig. 3). The majority of fibers are in the conventional beads-on-a-string morphology, revealing the linker DNA which is rarely seen in undepleted fibers. Thus, the presence of linker histones is required to maintain the three-dimensional structure of chromatin fibers even at low ionic strength.

SFM Images in Buffers Containing 10 mM NaCl. Thoma *et al.* (8) have suggested that an increase in salt concentration to 10 mM causes closing of the zig-zag to form a flat ribbon of nucleosomes. Attempts to image unfixed fibers at 10 mM

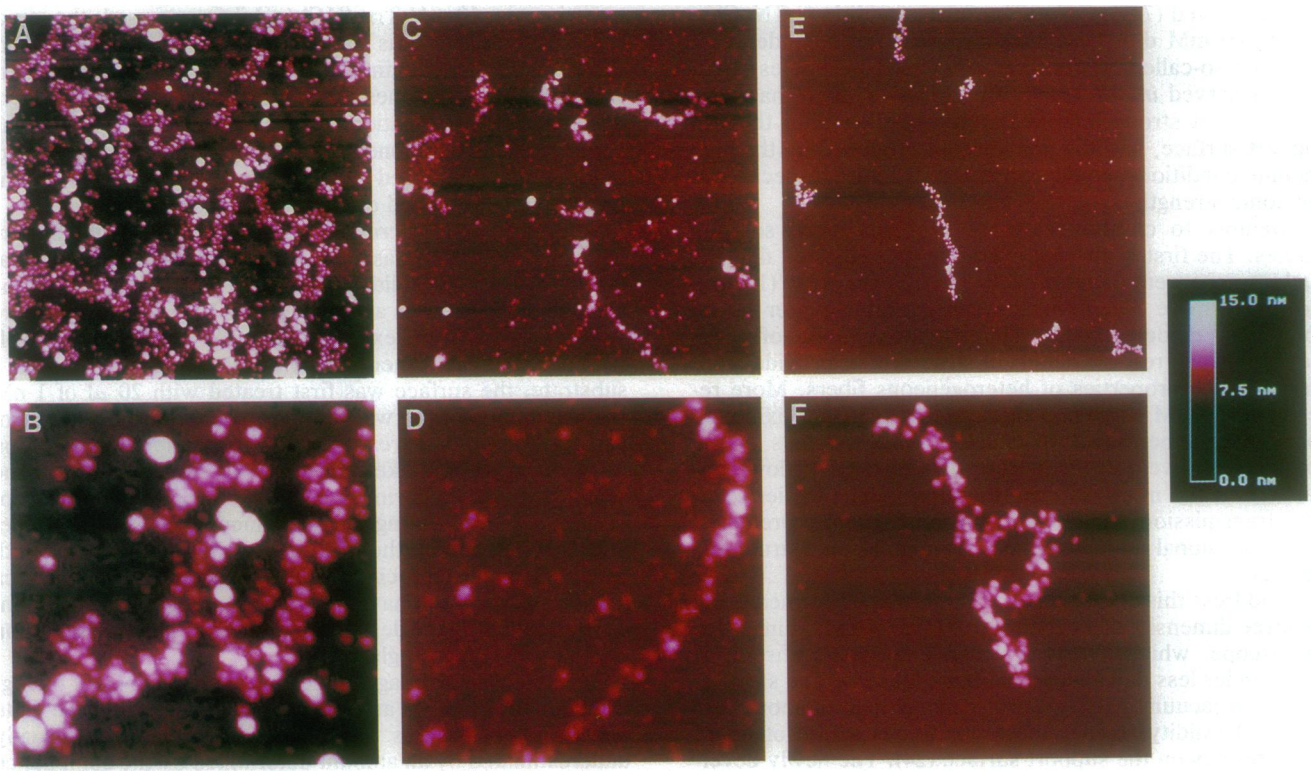

FIG. 1. Tapping-mode SFM images of unfixed (*A–D*) or glutaraldehyde-fixed (*E* and *F*) chromatin fibers deposited from 5 mM triethanolamine/HCl (pH 7.0) on glass (*A* and *B*) or mica (*C–F*). Image sizes are 2000 nm × 2000 nm (*A*, *C*, and *E*) and 600 nm × 600 nm (*B*, *D*, and *F*). Heights are coded by color, with low regions depicted in dark red and higher regions in increasingly lighter tones of red, as indicated in the height scale from 0 nm to 15 nm.

Table 1. Parameters of fibers as determined by SFM imaging

Conditions*	Apparent nucleosome diameter, nm	Apparent fiber diameter, nm	Corrected fiber diameter, nm	Minimal mass per length, no. of nucleosomes per 10 nm
Unfixed	16 ± 1	44 ± 5	34 ± 5	0.9 ± 0.15
Glutaraldehyde-fixed	12 ± 2	36 ± 4	34 ± 4	1.5 ± 0.25
10 mM NaCl, glutaraldehyde-fixed	10 ± 1	30 ± 5	30 ± 5	2.2 ± 0.35

Apparent diameters are a function of the properties of individual tips used in each series of experiments. Correction for tip dimensions is according to Eq. 1.
*Buffer was 5 mM triethanolamine/HCl (pH 7.0).

NaCl yielded only low-quality images on glass or resulted in extensive dissociation of the fibers on mica (see *Materials and Methods*).

Because of these difficulties, the conformation of chromatin fibers in 10 mM salt was studied after glutaraldehyde fixation. Glutaraldehyde fixation is known to maintain the structure of chromatin fibers even when, as here, the salt present at the time of fixation is removed afterwards (8, 10, 31) or when more salt is added (31). Further evidence that glutaraldehyde fixation does not cause gross artifacts is seen in Fig. 1: fixed and unfixed fibers, deposited from 5 mM triethanolamine/HCl (pH 7.0), are very similar in appearance.

Fibers fixed in 10 mM NaCl appeared better organized than those obtained in the absence of added salt, with some regions exhibiting what appears to be localized helical conformation (30). The fibers have a relatively uniform diameter of 30 ± 5 nm (Table 1).

Modeling of Chromatin Fibers at Low Salt. Recently, Woodcock *et al.* (32) proposed a model of the chromatin fiber in which the structure is dictated by a limited number of parameters, including the linker length and the angle between the DNA entering and exiting each nucleosome. If all linkers were of uniform length, a regular helix would result, but variability in linker length should produce an irregular, distorted helix.

A similar model, incorporating the values for linker lengths characteristic of chicken erythrocyte chromatin, can be used to predict an SFM image (Fig. 4). To do so, the computer-generated array of disk-shaped nucleosomes and DNA linkers was projected onto a surface; in such a projection each nucleosome touches either the surface or other nucleosomes already on the surface. The effects of finite tip dimensions on the image were then simulated according to the method of Keller and Franke (33). To make heights of nucleosomes in the calculated image agree with those actually observed in SFM, all heights were compressed by a factor of 2 as the imaginary tip scanned the model fiber. Clearly, as seen in Fig. 4, prediction and observation agree so well as to make blind guesses of which image is simulated and which is experimentally very difficult.

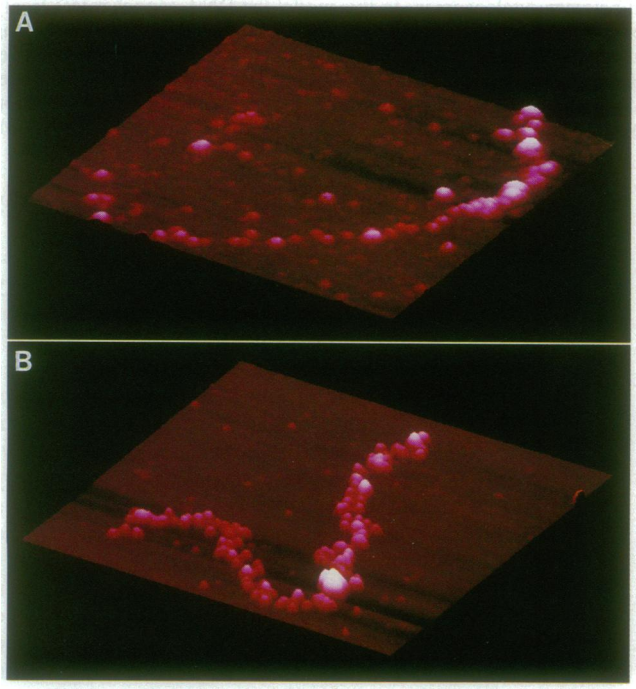

FIG. 2. SFM images of unfixed (*A*) or fixed (*B*) chromatin fibers deposited from 5 mM triethanolamine HCl (pH 7.0) on mica and viewed from an inclination angle of 30°. In *A* (the same molecule is depicted in Fig. 1*D*), a rare example of a transition between a structured fiber and an extended string of nucleosomes is shown. These transitions were observed only in unfixed samples. Image sizes are 600 nm × 600 nm. Heights are coded as in Fig. 1, with a scale from 0 nm to 30 nm.

DISCUSSION

Integrity of Samples. A concern in any *in vitro* study of chromatin structure is the integrity of the samples. The materials used here were carefully monitored by all available criteria. The digestions to prepare long fibers were mild, with samples never exposed to salt concentrations above 150 mM. Gel electrophoresis indicated that all histones were present in

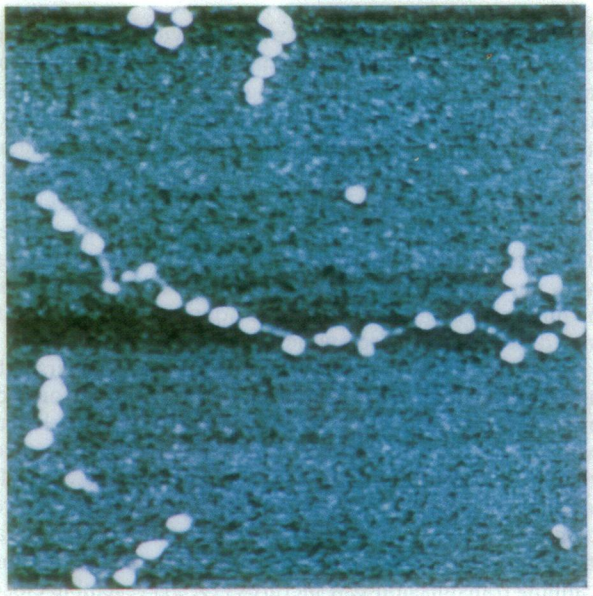

FIG. 3. SFM image of fibers which had been stripped of the linker histones, fixed, and then deposited from 5 mM triethanolamine/HCl (pH 7.0) on mica. Image size is 600 nm × 600 nm. The color of the height scale (0 nm to 12 nm from dark blue to white) has been changed to facilitate the visualization of the linker DNA.

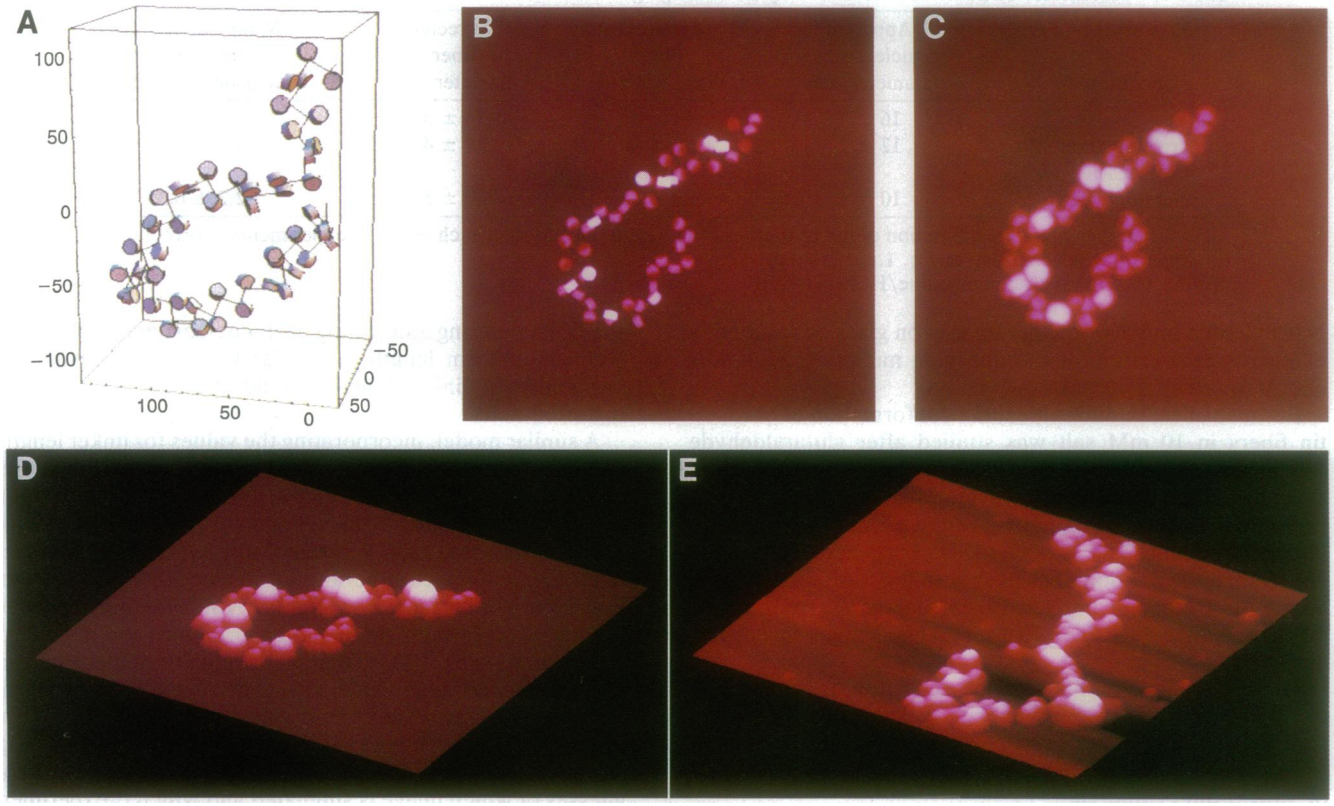

FIG. 4. Model of the chromatin fiber and its simulated SFM image. (*A*) Model of a chromatin fiber used in these simulations. The DNA wraps in a left-handed fashion 1.75 turns around a histone octamer. The octamer is simulated by a disk 5.5 nm high and 11 nm in diameter. The radius of curvature of the DNA wrapped around the core is 55 Å, and the pitch of the DNA is 28.6 Å. The DNA has 10.15 bp per turn around the histone octamer and 10.4 bp per turn in the linker portion. The exit angle of the DNA is determined by the tangent at the point it leaves the nucleosome. The length of the linker DNA is determined by means of a uniform deviate random-number algorithm which generates linker lengths between 60 and 64 bp. The linker DNA is assumed to adopt a straight configuration between nucleosomes. In this model the DNA cannot rotate freely on the surface of the nucleosome core. This feature simulates the DNA–core interactions which fix the DNA–octamer surface contacts along the path of the DNA. This model generates three-dimensional, randomly organized fibers with an average diameter of 30 nm. (*B*) The model in *A* as it appears on a plane after partial flattening to simulate the process of deposition on the mica. (*C*) Simulated SFM image of the model in *B*, obtained by convoluting this model with a parabolic tip with a radius of curvature of 10 nm. (*D*) Image of *C* viewed from a 30° inclination angle. (*E*) A 30° view of an experimental SFM image of a fixed chromatin fiber deposited on mica from 5 mM triethanolamine/HCl (pH 7.0). Image sizes are 400 nm × 400 nm (*B–E*). Heights are coded as in Fig. 1, with a scale from 0 nm to 50 nm.

their normal stoichiometries, with no evidence of degradation. Samples prepared by this method condense into compact fibers at higher ionic strength (30), and also become highly resistant to attack by micrococcal nuclease (28), a further indication of compaction. The ability to condense may serve as an indication for the integrity of the samples, since even slight damage to the linker histones would affect this property (e.g., ref. 34). Although none of these criteria (nor any other known criterion) can guarantee that each and every chromatin fiber is intact, they reflect the properties of the dominant forms present in the population, which are the ones described in these studies.

Comparison with Other Results. In terms of general fiber morphology, none of the scattering experiments performed at low ionic strength have been consistent with a linearly extended, beads-on-a-string structure but could be consistent with the kind of irregular fibers seen in the present study. The flattened zig-zag conformation in EM images may result from strong interactions of the fibers with the supporting surface and complete removal of water of hydration. However, some scanning transmission EM pictures (19, 21) resemble closely what would be expected for two-dimensional projections of the kind of structures observed here.

The average radii of the fibers are in the range 30–40 nm. Very similar values have been estimated from studies of chromatin in dilute aqueous salt solutions using light scattering (13, 14), electric birefringence (15), or low-angle x-ray scattering (16, 35).

Mass-per-unit-length measurements from solution studies typically indicate one to two nucleosomes per 10 nm at very low salt (11, 12, 18), increasing to two to three nucleosomes per 10 nm with the addition of NaCl to 20 mM (12). Direct counting of individual nucleosomes on many SFM images yielded the values given in Table 1. These are *minimal* estimates because only nucleosomes on top of the fibers can be counted, while it is clear that some are hidden below. Thus, the actual values are likely to be larger, but surely <2-fold greater. The data in Table 1 show that a moderate increase in ionic strength leads to an axial contraction of the fiber without significant change in radius.

Fibers as Distorted Helices. The modeling studies provide a credible rationale for the observed structures. Given the constraints imposed, a chain of nucleosomes must have the kind of quasi-order observed in the SFM pictures. Relaxation of any of those constraints can be expected to lead to different conformations. For example, removal of lysine-rich histones relaxes the restriction on exit and entry angles of DNA in the nucleosome, thereby allowing the extended beads-on-a-string structure, as observed here and in another recent SFM study of oligonucleosomes reconstituted in the absence of linker histones (36). With increasing ionic strength the linkers should become more flexible (37) and nucleosome–

nucleosome interactions should become stronger. Both these effects should lead to axial contraction of the fiber without gross changes in fiber morphology, exactly as is observed in the salt concentration range studied here. Ionic strength-dependent compaction of dinucleosomes has been directly demonstrated (38). The marked condensation of chromatin observed at still higher ionic strengths may require more fundamental changes in the structure. The observation that the location of lysine-rich histones with respect to the nucleosomes is different under low and high ionic strength conditions (26) may provide a key to this condensation.

We thank Dr. J. P. Langmore for advice, Drs. E. Trifonov and D. Erie for discussion, and V. Stanik for technical assistance. This research was supported by National Institutes of Health Research Grants GM22916 (K.v.H.), and GM32543 (C.B.), National Science Foundation Grant BIR 9318945 (C.B.), a grant of the Lucille P. Markey Charitable Foundation to the Institute of Molecular Biology (University of Oregon), and a National Institutes of Health Postdoctoral Fellowship GM16600 (S.H.L.).

1. Miller, O. L., Jr., & Bakken, A. H. (1972) *Acta Endocrinol. Suppl.* **168,** 155–177.
2. Olins, A. L. & Olins, D. E. (1974) *Science* **183,** 330–332.
3. Woodcock, C. L. F. (1973) *J. Cell Biol.* **59,** 368 (abstr.).
4. van Holde, K. E. (1988) *Chromatin* (Springer, New York).
5. Thoma, F. (1988) in *Architecture of Eurkaryotic Genes*, ed. Kahl, G. (VCH, Weinheim, Germany), pp. 163–185.
6. Tsanev, R., Russev, G., Pashev, I. & Zlatanova, J. (1992) *Replication and Transcription of Chromatin* (CRC, Boca Raton, FL).
7. Thoma, F. & Koller, T. (1977) *Cell* **12,** 101–107.
8. Thoma, F., Koller, T. & Klug, A. (1979) *J. Cell Biol.* **83,** 403–427.
9. Thoma, F. & Koller, T. (1981) *J. Mol. Biol.* **149,** 709–733.
10. De Murcia, G. & Koller, T. (1981) *Biol. Cell* **40,** 165–174.
11. Sperling, L. & Tardieu, A. (1976) *FEBS Lett.* **64,** 89–91.
12. Suau, P., Bradbury, E. M. & Baldwin, J. P. (1979) *Eur. J. Biochem.* **97,** 593–602.
13. Campbell, A. M., Cotter, R. I. & Pardon, J. F. (1978) *Nucleic Acids Res.* **5,** 1571–1580.
14. Marion, C., Bezot, P., Hesse-Bezot, C., Roux, B. & Bernengo, J.-C. (1981) *Eur. J. Biochem.* **120,** 169–176.
15. Marion, C. (1984) *J. Biomol. Struct. Dyn.* **2,** 303–316.
16. Perez-Grau, L., Bordas, J. & Koch, M. H. J. (1984) *Nucleic Acids Res.* **12,** 2987–2996.
17. Bordas, J., Perez-Grau, L., Koch, M. H. J., Vega, M. C. & Nave, C. (1986) *Eur. Biophys. J.* **13,** 157–173.
18. Bordas, J., Perez-Grau, L., Koch, M. H. J., Vega, M. C. & Nave, C. (1986) *Eur. Biophys. J.* **13,** 175–185.
19. Gerchman, S. E. & Ramakrishnan, V. (1987) *Proc. Natl. Acad. Sci. USA* **84,** 7802–7806.
20. Swerdlow, J. R., Agard, D. A. & Sedat, J. W. (1993) *Curr. Opin. Cell Biol.* **5,** 412–416.
21. Woodcock, C. L. F., Frado, L.-L. Y. & Rattner, J. B. (1984) *J. Cell Biol.* **99,** 42–52.
22. Binnig, G., Quate, C. F. & Gerber, C. (1986) *Phys. Rev. Lett.* **56,** 930–933.
23. Bustamante, C., Keller, D. & Yang, G. (1993) *Curr. Opin. Struct. Biol.* **3,** 363–372.
24. Grigg, D. A., Russell, P. E. & Griffith, J. E. (1992) *J. Vac. Sci. Technol. A* **10,** 680–683.
25. Thompson, M. (1993) *Digital Instruments Nanotips* (Digital Instruments, Santa Barbara, CA).
26. Bavykin, S. G., Usachenko, S. I., Zalensky, A. O. & Mirzabekov, A. D. (1990) *J. Mol. Biol.* **212,** 495–511.
27. Yager, T. D., McMurray, C. T. & van Holde, K. E. (1989) *Biochemistry* **28,** 2271–2281.
28. Leuba, S. H., Zlatanova, J. & van Holde, K. (1994) *J. Mol. Biol.* **235,** 871–880.
29. Libertini, L. J. & Small, E. W. (1980) *Nucleic Acids Res.* **8,** 3517–3534.
30. Zlatanova, J., Leuba, S. H., Yang, G., Bustamante, C. & van Holde, K. (1994) *Proc. Natl. Acad. Sci. USA* **91,** 5277–5280.
31. Russanova, V. R., Dimitrov, S. I., Makarov, V. L. & Pashev, I. G. (1987) *Eur. J. Biochem.* **167,** 321–326.
32. Woodcock, C. L., Grigoryev, S. A., Horowitz, R. A. & Whitaker, N. (1993) *Proc. Natl. Acad. Sci. USA* **90,** 9021–9025.
33. Keller, D. J. & Franke, F. S. (1993) *Surf. Sci.* **294,** 409–419.
34. Leuba, S. H., Zlatanova, J. & van Holde, K. (1993) *J. Mol. Biol.* **229,** 917–929.
35. Williams, S. P., Athey, B. D., Muglia, L. J., Schappe, R. S., Gough, A. H. & Langmore, J. P. (1986) *Biophys. J.* **49,** 233–248.
36. Allen, M. J., Dong, X. F., O'Neill, T. E., Yau, P., Kowalczykowski, S. C., Gatewood, J., Balhorn, R. & Bradbury, E. M. (1993) *Biochemistry* **32,** 8390–8398.
37. Hagerman, P. J. (1988) *Annu. Rev. Biophys. Biophys. Chem.* **17,** 265–286.
38. Yao, J., Lowary, P. T. & Widom, J. (1990) *Proc. Natl. Acad. Sci. USA* **87,** 7603–7607.